Available online at www.sciencedirect.com
ScienceDirect
Biochimica et Biophysica Acta 1777 (2008) 343–350
Biochimica et Biophysica Acta BBA
www.elsevier.com/locate/bbabio

Deuterium isotope effect of proton pumping in cytochrome *c* oxidase

Lina Salomonsson [1], Gisela Brändén [1], Peter Brzezinski *

Department of Biochemistry and Biophysics, The Arrhenius Laboratories for Natural Sciences, Stockholm University, SE-106 91 Stockholm, Sweden

Received 5 June 2007; received in revised form 11 September 2007; accepted 20 September 2007
Available online 6 October 2007

Abstract

In mitochondria and many aerobic bacteria cytochrome *c* oxidase is the terminal enzyme of the respiratory chain where it catalyses the reduction of oxygen to water. The free energy released in this process is used to translocate (pump) protons across the membrane such that each electron transfer to the catalytic site is accompanied by proton pumping. To investigate the mechanism of electron–proton coupling in cytochrome *c* oxidase we have studied the pH-dependence of the kinetic deuterium isotope effect of specific reaction steps associated with proton transfer in wild-type and structural variants of cytochrome *c* oxidases in which amino-acid residues in proton-transfer pathways have been modified. In addition, we have solved the structure of one of these mutant enzymes, where a key component of the proton-transfer machinery, Glu286, was modified to an Asp. The results indicate that the $P^3 \rightarrow F^3$ transition rate is determined by a direct proton-transfer event to the catalytic site. In contrast, the rate of the $F^3 \rightarrow O^4$ transition, which involves simultaneous electron transfer to the catalytic site and is characteristic of any transition during Cyt*c*O turnover, is determined by two events with similar rates and different kinetic isotope effects. These reaction steps involve transfer of protons, that are pumped, *via* a segment of the protein including Glu286 and Arg481.

Keywords: Cytochrome aa3; Electron transfer; Proton transfer; Membrane protein; Transmembrane transport; Kinetics; Spectroscopy; Mitochondria

1. Introduction

Cytochrome *c* oxidase (Cyt*c*O), the terminal enzyme of the respiratory chain in many aerobic organisms, couples the energy released upon electron transfer to oxygen to translocation of protons across the inner mitochondrial or cell membrane. The electrochemical proton gradient that is formed is used, for example, to produce ATP (for recent reviews, see [1–10]).

In Cyt*c*O (cytochrome aa_3) from *Rhodobacter* (*R.*) *sphaeroides*, electrons are donated one at a time by a water-soluble cytochrome *c* from the more positive (*P*) side of the membrane, *via* a dinuclear copper center (Cu_A), to heme *a* and then onto the catalytic site, composed of heme a_3 and a copper ion (Cu_B) (see Fig. 1A). Each electron transfer is linked to the uptake of a substrate proton from the more negative (*N*) side of the membrane. In addition, each electron and proton transfer to the catalytic site is coupled to pumping of one proton from the *N*-side to the *P*-side, across the membrane. In Cyt*c*O from *R. sphaeroides* there are two distinct proton pathways leading from the *N*-side surface to the catalytic site, the D and K pathways [11–13]. In addition, a third pathway, the H pathway, has been identified and suggested to be unique for the mitochondrial Cyt*c*O [14]. The K pathway is used exclusively during reduction of Cyt*c*O to transfer ~2 protons, while the D pathway is used for the transfer of the remaining ~6 protons, i.e. both substrate protons and protons to be pumped [15–17]. The branching point in the D pathway from where protons are transferred either to the catalytic site or an acceptor for pumped protons is presumably located at Glu286 of subunit I (E286), at the end of the D pathway. The acceptor of pumped protons beyond E286 is not known, but several candidates have been discussed based on results from experimental and theoretical work. One such candidate is a cluster including the heme a_3 D-propionate and Arg481/Arg482 [11,18–23], while other candidates include an Asp residue near the *P*-side surface of subunit I [24] or one of the His ligands of Cu_B [25,26].

* Corresponding author. Fax: +46 8 153679.
E-mail address: peterb@dbb.su.se (P. Brzezinski).
[1] The authors have contributed equally.

0005-2728/$ - see front matter © 2007 Elsevier B.V. All rights reserved.
doi:10.1016/j.bbabio.2007.09.009

The catalytic cycle of Cyt*c*O is depicted in Fig. 1B [27], which shows the different intermediate states of the enzyme denoted by one-letter codes, where the total number of electrons transferred to the catalytic site is given by the superscript. Oxygen binds to the two-electron reduced catalytic site (state R^2), forming state A^2. Upon binding of O_2 to heme a_3 the O–O-bond is broken, which results in formation of state P^2 (also called P_M). Transfer of the third and fourth electron is each accompanied by proton uptake, forming the F^3- and O^4-states, respectively. If the enzyme is instead pre-loaded with four electrons so that also Cu_A and heme *a* are reduced when initiating the reaction, an electron is transferred from heme *a* to the catalytic site upon O_2-bond cleavage, forming state P^3 (also called P_R). The P^3-state carries one additional electron as compared to the P^2-state discussed above. Formation of the next state, F^3, is thus associated with proton transfer only. In the last step, the O^4-state is formed upon electron and proton transfer to the catalytic site. Each of the transitions $P^2/P^3 \rightarrow F^3$ and $F^3 \rightarrow O^4$ is coupled to pumping of one proton [28–31].

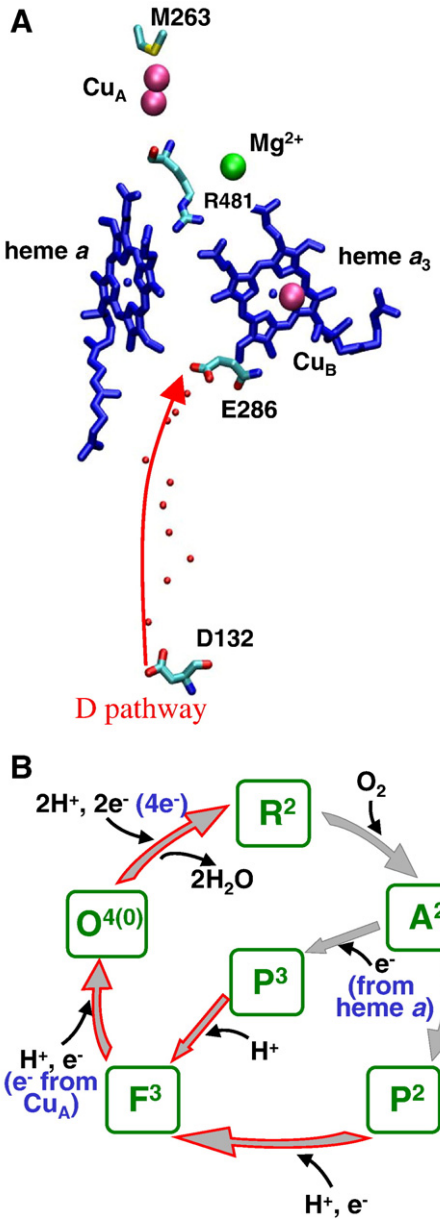

Fig. 1. (A) Cu_A, heme *a*, heme a_3, Cu_B, and the residues investigated or discussed in this study. The D proton pathway is indicated with an arrow, and water molecules are shown in red. (B) A reaction cycle of Cyt*c*O, where the two- or four-electron reduced enzyme reacts with O_2. For simplicity the Cu_A and heme *a* sites are not shown. The different transitions are described in the text. The superscripts indicate the number of electrons transferred to the catalytic site in each state. In the sequence of events during Cyt*c*O turnover the oxidized Cyt*c*O receives first two electrons after which O_2 binds to heme a_3 (the outer circle). The remaining two electrons are added one by one from an external donor. In the experiments in this study the Cyt*c*O was initially reduced by four electrons (i.e. in addition to the catalytic site also Cu_A and heme *a* are reduced) and the reaction proceeds through the P^3-state (see blue text). Transitions associated with pumping are indicated with gray/red arrows.

In each of the transitions $P^2/P^3 \rightarrow F^3$ and $F^3 \rightarrow O^4$ proton transfer to the catalytic site occurs *via* the D pathway where in each step E286 is transiently deprotonated followed by reprotonation from solution [32]. The apparent pK_a of E286, determined from the pH dependence of the $P^3 \rightarrow F^3$ rate, is 9.4 [33]. Even though Fourier Transform Infrared Spectroscopy (FTIR) data show no perturbation of the E286 residue in some of the states discussed above [34,35] (see also [36]), the FTIR data is not inconsistent with the involvement of E286 as a proton donor/acceptor because in each of the transitions E286 is rapidly reprotonated from solution [33]. In other words, E286 is only transiently deprotonated during the transition and it is protonated before and after the reaction.

A valuable tool that can be used to obtain information on the proton-transfer reactions in Cyt*c*O is investigation of the solvent kinetic deuterium isotope effects (KIEs) of the different reaction steps, i.e. to compare the rates of specific transitions in H_2O and D_2O, respectively. A relatively small KIE (~1.4) is expected for a direct proton transfer from a donor to an acceptor connected by hydrogen bonds, whereas if proton tunneling or conformational changes are involved, the KIE might be much larger [37,38]. It has been shown previously that the $P^3 \rightarrow F^3$ transition of Cyt*c*O from *R. sphaeroides* displays a KIE of ~2.5, while the $F^3 \rightarrow O^4$ transition displays a larger KIE of 5–7 [39] (see also [40]), presumably because of different rate-limiting steps of these transitions. The single-electron reduction of compound F (to form state O) has also been shown to display a KIE of 4–8 [41–43]. The large KIE of the $F^3 \rightarrow O^4$ transition has been attributed to a structural rearrangement that is linked to the release of a pumped proton or the proton release itself [44,45].

Here, we present an investigation of the pH-dependences of the KIEs of specific reaction steps in the wild-type as well as in mutant forms of Cyt*c*O: ED286, DN132 and RK481. The modified residues have been shown previously to be involved in proton transfer reactions during O_2-reduction (reviewed in [3,10,27]). The aim of the study was to compare changes in magnitude of the KIEs in the wild-type and mutant Cyt*c*Os to identify the structure–function relation rather than to explain the origin of the isotope effects themselves in terms of molecular mechanisms, which is a much more complex problem. The results identify the rate-limiting steps of the different reaction steps and point to a specific region of the protein that might be involved in controlling proton pumping.

2. Materials and methods

2.1. Enzyme preparation

Histidine-tagged mutant and wild-type Cyt*c*O were purified from *R. sphaeroides* as previously described, and the concentration was determined using UV-visible absorption spectroscopy [46]. Mutant strains of Cyt*c*O were obtained from R.B. Gennis (DN132 [47], ED286, [22]) and S. Ferguson-Miller (RK481, [48]).

2.2. Preparation of the fully reduced CO-bound CytcO

The Cyt*c*O buffer was exchanged on a PD-10 column (Amersham Biosciences) for 100 mM KCl, 0.1% DDM (n-dodecyl-*β*-D-maltoside) at pH/pD 7.5, with a final enzyme concentration of 10 μM. H_2O was exchanged for D_2O (99%) by concentration and re-dilution using Microcon YM-100 filters (Amicon) until the residual amount of H_2O was 2–5%. The sample was transferred to an anaerobic cuvette, which was repeatedly evacuated on a vacuum line and flushed with N_2 gas. The Cyt*c*O was reduced with 5 mM ascorbate and 0.2 μM phenazine methosulphate (redox mediator), and the N_2 was exchanged for CO.

2.3. Flow-flash kinetic measurements

The Cyt*c*O–CO complex was rapidly mixed at a 1:5 ratio with an O_2-saturated buffer-solution in a stopped-flow apparatus. The pH/pD after mixing was set by the O_2-saturated buffer solution, which contained one of the buffers MES, HEPES–KOH, Tris–HCl, CHES, CAPS or CABS (each at a concentration of 100 mM), depending on the pH/pD, and 0.1% DDM. Thus, the enzyme was exposed only for seconds to the new pH value, which allowed us to perform studies also at pH-values approaching those where the enzyme becomes unstable [33]. The time between mixing and the flash (i.e. the initiation of the experiment) was sufficient to allow the enzyme solution to equilibrate with the new pH [33]. For the measurements with the DN132 mutant Cyt*c*O the enzyme was pre-incubated in the buffer of the appropriate pH/pD because in this mutant Cyt*c*O protons equilibrate slowly with the enzyme interior through the D pathway. About 300 ms after mixing, the CO ligand was dissociated using a short laser flash at 532 nm (Quantel, Brilliant B), and the reaction was monitored by recording the absorbance changes at 445 nm and 580 nm. The locally modified flow-flash apparatus (Applied Photophysics, Leatherhead Surrey, UK) used in these measurements is described in more detail in [49]. The data were analyzed using the PRO-K software (Applied Photophysics).

The pH-dependence measurements were performed at the equivalent pH or pD values in order to keep the same proton concentration when comparing rates obtained in H_2O with those obtained in D_2O.

2.4. Structural analysis by X-ray crystallography

The structure of the ED286 mutant Cyt*c*O was determined using X-ray crystallography. Crystals were prepared as described for the *R. sphaeroides* wild-type enzyme [12], and low-temperature data collection was carried out at beam line ID14-2 at the European Synchrotron Radiation Facility (ESRF, http://www.esrf.fr). The crystals of space group R3, cell dimensions 339.6, 339.6, 90.2 Å, 90, 90, 120°, diffracted up to 3.0 Å in the a* and b* axis plane and up to 3.5 Å in the c* axis plane (anisotropic diffraction). The data were integrated and scaled using the HKL program suite [50] with the following statistics: number of reflections 122298, unique reflections 69336, I/σ(I) 7.9, completeness 89.4%, R-merge 6.1%. The structure was refined using the rigid body refinement program in REFMAC with the wild-type Cyt*c*O structure (PDB coordinates 1M56) as a starting model [51]. Due to the limited resolution, water molecules were not included in the model. The *R*-value and free *R*-value after TLS refinement with two TLS-groups per asymmetric unit was 26.3 and 28.1, respectively.

3. Results

The kinetics of the $P^3 \rightarrow F^3$ and $F^3 \rightarrow O^4$ transitions was determined by measuring absorbance changes at 580 nm and 445 nm as a function of time after flash-induced dissociation of CO from the fully reduced Cyt*c*O in the presence of O_2 (flow-flash technique, see Materials and methods). Proton pumping occurs on the same time scales as the $P^3 \rightarrow F^3$ and $F^3 \rightarrow O^4$ transitions but cannot be directly observed spectroscopically. Typical traces obtained with the wild-type Cyt*c*O are shown in [18,33].

3.1. Kinetic deuterium isotope effect in wild-type CytcO

The $P^3 \rightarrow F^3$ transition rate in wild-type Cyt*c*O was determined in the pH or pD range between 6 and 12 by measuring absorbance changes at 580 nm. As shown previously, the pH dependence of the rate in H_2O could be well fitted to a Henderson–Hasselbalch titration curve displaying a pK_a of 9.4 and a maximum rate of $\sim 1.1 \cdot 10^4$ s^{-1} at low pH (Fig. 2A and [33]). This pK_a value was attributed to the residue E286, but it should be noted that the value is determined from the kinetics of the $P^3 \rightarrow F^3$ transition, which means that it is only an apparent value (the same applies to the other pK_a values discussed in this work). In D_2O the pK_a was shifted slightly to 9.6, and the maximum rate of the transition was 5000 s^{-1} (Fig. 2A). The KIE for the $P^3 \rightarrow F^3$ transition, in the pH-independent region, is ~2.2 in agreement with previous results obtained at pH 7.5 [39].

As shown previously the pH dependence of the $F^3 \rightarrow O^4$ reaction rate in H_2O is determined by the protonation state of two groups with pK_as of <6 and 8.9, respectively. The transition rate constant is ~1000 s^{-1} at pH 6 and the minimum rate at high pH is ~150 s^{-1} (Fig. 2B and [18,52]). In contrast, in D_2O the $F^3 \rightarrow O^4$ transition rate displayed a distinctly different behavior, with a pH-dependence that could be fitted to a titration curve with a pK_a of 6.7 (Fig. 2B). This phase displayed a maximum rate of ~250 s^{-1}, and a minimum rate of ~50 s^{-1}. The KIE for the $F^3 \rightarrow O^4$ transition was 4–7 in the pH range 6–9, with a value of ~6 at pH 7.5.

3.2. Kinetic isotope effects in DN132, ED286 and RK481 mutant CytcOs

The KIEs for the $P^3 \rightarrow F^3$ and $F^3 \rightarrow O^4$ transitions were investigated in structural variants of Cyt*c*O where the key components E286, D132 and R481 (see Fig. 1A) along the proton-transfer trajectory were modified. The results are summarized in Table 1.

Asp132 is located at the entrance of the D pathway, and upon mutation of this residue to a non-protonatable Asn (DN132), proton uptake is dramatically slowed and proton pumping is impaired [53]. The rate of the $P^3 \rightarrow F^3$ transition is not affected by the slowed proton uptake because the proton needed to form F^3 is taken internally from E286 [32]. The KIE of the $P^3 \rightarrow F^3$ transition (i.e. proton transfer from E286 to the catalytic site) at pH 7.5 with the DN132 mutant Cyt*c*O was ~2, i.e. similar to the KIE with wild-type enzyme (not shown). The $F^3 \rightarrow O^4$ transition involves proton uptake from solution and it is therefore dramatically slowed in the DN132 mutant Cyt*c*O to 1.6 s^{-1} (at pH 7.5). The KIE of this rate was small (~1.6 at pH 7.5, see Fig. 2C). The rate did not reach a maximum below pH

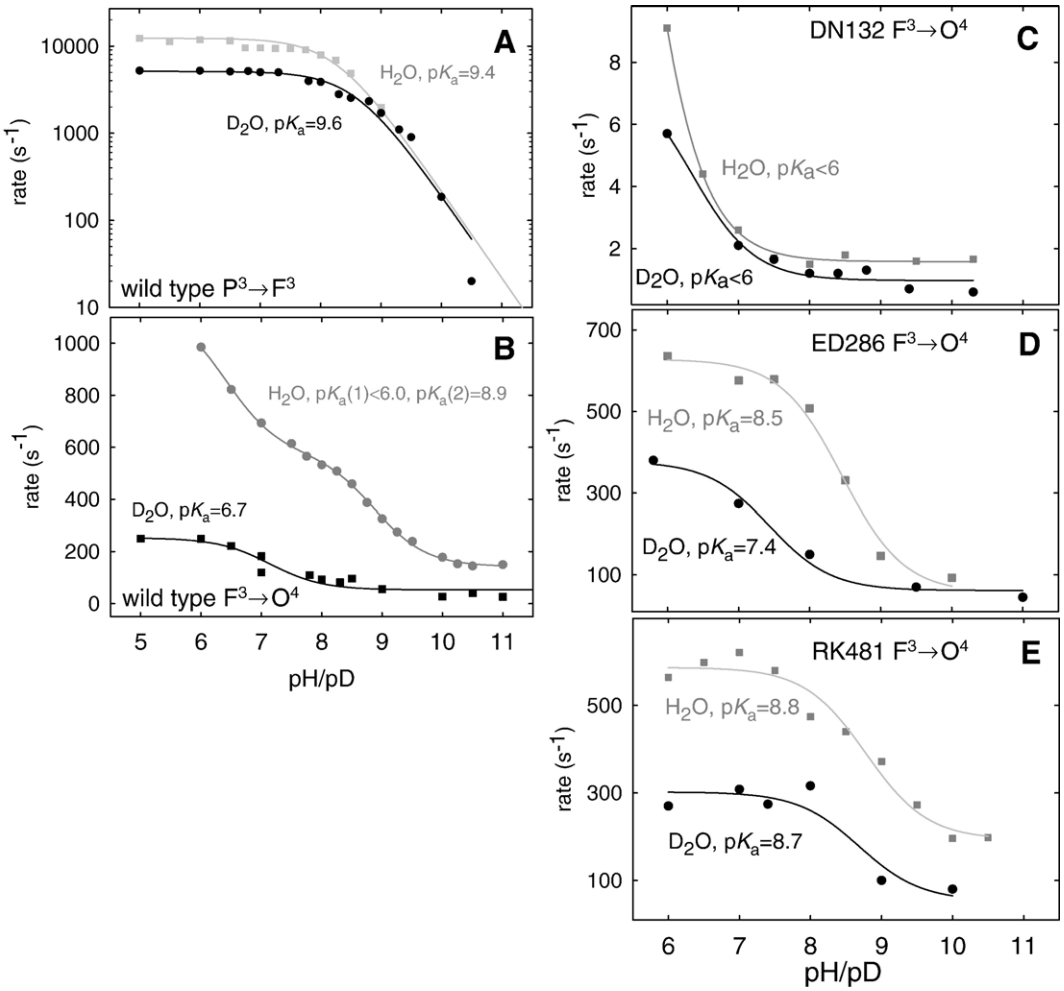

Fig. 2. The pH-dependence of the $P^3 \rightarrow F^3$ transition rates with wild-type (A) (the H_2O data are from [33]), and $F^3 \rightarrow O^4$ transition rates with wild-type (the H_2O data are from [18]) (B), DN132 mutant (C), ED286 mutant (D), and RK481 mutant (E) Cyt*c*Os, in H_2O (gray squares) and D_2O (black circles) during reaction of the fully reduced enzyme with O_2. The gray (H_2O) and black (D_2O) lines are fits of the data with standard titration curves. The transition rates were obtained from traces at 580 nm and 445 nm with (A) pK_a=9.4 (H_2O) and pK_a=9.6 (D_2O), (B) $pK_a(1)<$, $pK_a(2)$=8.9 (H_2O) and pK_a=6.7 (D_2O), (C) $pK_a<6$ in both H_2O and D_2O, (D) pK_a=8.5 (H_2O) and pK_a=7.4 (D_2O), (E) pK_a=8.8 (H_2O) and pK_a=8.7 (D_2O). Experimental conditions: ~2 μM reacting enzyme, 0.1 M MES, HEPES–KOH, Tris–HCl, CHES, CAPS or CABS, 0.1% DDM, 1 mM O_2, and 22 °C.

6, indicating a pK_a <6 in both H_2O and D_2O, which might reflect an alternative proton acceptor/donor at the entrance of the D pathway such as e.g. His26 [54] or His549 [55].

The ED286 mutant in *R. sphaeroides* Cyt*c*O has a 50% oxygen-reduction activity of that of the wild-type Cyt*c*O, and pumps protons with the same stoichiometry as the wild-type Cyt*c*O (~1 H^+/e^-) in H_2O as well as in D_2O (not shown). In H_2O at pH 7.8 the $P^3 \rightarrow F^3$ and $F^3 \rightarrow O^4$ transitions are slowed by factors of ~5 and ~2.5, respectively (as compared to the corresponding rates with the wild-type Cyt*c*O), i.e. the $F^3 \rightarrow O^4$ transition is retarded to a lesser extent than the $P^3 \rightarrow F^3$ transition [22]. The KIE of the $P^3 \rightarrow F^3$ transition at pH 7.5 was ~2.5 with the ED286 mutant Cyt*c*O, which is similar to the KIE with wild-type enzyme (not shown). The pH-dependence of the $F^3 \rightarrow O^4$ transition in H_2O and D_2O is shown in Fig. 2D. The traces could be fitted with a Henderson–Hasselbalch titration curve displaying pK_as of 8.5 and 7.4 in H_2O and D_2O, respectively. The KIE of this transition was ~2.5 (at pH 7.5), i.e. smaller than that observed with the wild-type Cyt*c*O (KIE≅6) [22].

In the RK481 mutant Cyt*c*O the D-ring propionate of heme a_3 presumably has an altered pK_a due to the replacement of the nearby Arg481 by a Lys [18]. The $P^3 \rightarrow F^3$ transition of the RK481 mutant Cyt*c*O displayed a KIE of ~2.1, similar to that observed with the wild-type Cyt*c*O (not shown). The pH-dependence of the $F^3 \rightarrow O^4$ transition rate for the RK481 mutant

Table 1
The rates and, KIEs and pK_as associated with the $P^3 \rightarrow F^3$ and $F^3 \rightarrow O^4$ transitions in Cyt*c*O from *R. sphaeroides* (the errors in the pK_a values are 5% and the errors in the KIE values are 15%)

	pK_a $F^3 \rightarrow O^4$		KIE at pH≅7.5		$P^3 \rightarrow F^3$ rate (ms^{-1})		$F^3 \rightarrow O^4$ rate (s^{-1})	
	H_2O	D_2O	$P^3 \rightarrow F^3$	$F^3 \rightarrow O^4$	H_2O	D_2O	H_2O	D_2O
WT	≤6.4 & 8.9	6.7	2.2	5.6	11	5.0	614	110
DN132	≤6	≤6	2.0	1.6	10.0	5.0	1.6	1.0
ED286	8.5	7.4	2.5	2.5	1.2	0.48	580	230
RK481	8.8	8.7	2.1	2.3	11	5.3	660	280

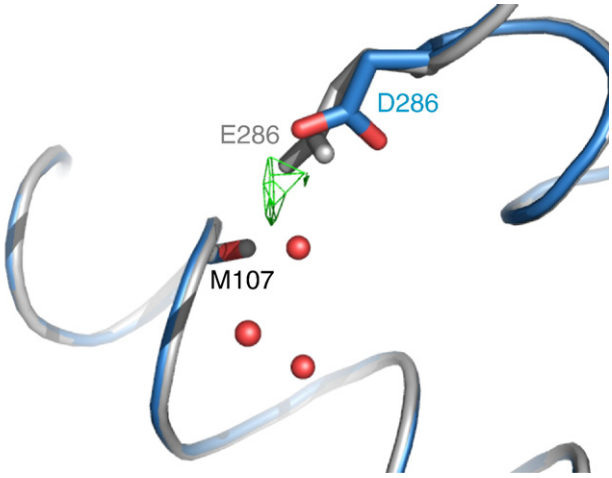

Fig. 3. The structure of the ED286 mutant (blue) overlaid on that of the wild-type (WT, gray) Cyt*c*O (PDB-entry 1M56, [12]). Water molecules in the wild-type Cyt*c*O structure are shown in red. The difference electron density for the mutant enzyme is shown in green at a cut-off of 2.6 sigma.

Cyt*c*O displayed pK_as of 8.8 and 8.7 in H_2O and D_2O, respectively (Fig. 2E). The KIE was about 2.3 (at pH 7.5), i.e. smaller than that observed with the wild-type Cyt*c*O.

The low-pK_a (<6) titration of the $F^3 \rightarrow O^4$ transition, seen with the wild-type Cyt*c*O in H_2O (Fig. 2B), was not observed with the ED286 or RK481 mutant Cyt*c*Os, which may explain the smaller KIEs in these mutants (see Discussion).

3.3. Structure of the ED286 mutant CytcO

The X-ray crystal structure of the ED286 mutant Cyt*c*O indicates that the shorter side chain of D286 compared to that of E286 leaves a pocket with enough space for an additional water molecule in the mutant enzyme (see Fig. 3). Due to the limited resolution of the mutant Cyt*c*O structure (3.0/3.5 Å), water molecules were not included in the refinement. However, in the difference Fourier electron density map (shown as a green mesh in Fig. 3) there is a peak between the D286 side chain and the water molecule hydrogen-bonded to E286 in the wild-type structure. This electron density could correspond to a new water molecule, or alternatively, the reallocation of one already present in wild-type Cyt*c*O. We also see that the hydrogen bond between residue 286 and the carbonyl oxygen of M107, observed in the wild-type Cyt*c*O, is not present in the ED286 mutant Cyt*c*O structure as the distance is too large.

4. Discussion

We have studied the pH-dependencies of the transition rates during reaction of the fully reduced Cyt*c*O with O_2 in H_2O and D_2O. A comparison of the KIEs in the wild-type and structural variants of the enzyme in which residues along the proton-transfer trajectory have been modified provides information on the rate-determining steps and structural elements involved in controlling proton-transfer rates in Cyt*c*O.

4.1. The $P^3 \rightarrow F^3$ transition

The $P^3 \rightarrow F^3$ transition does not involve simultaneous intramolecular electron transfer (the electron needed to form F^3 is transferred to the catalytic site already during formation of P^3) and it is only associated with proton transfer. Previous observations have shown that the $P^3 \rightarrow F^3$ transition rate displays a KIE of ~2 [39], which is attributed to proton uptake, through the D pathway, to the catalytic site [44]. Because most likely the rate-limiting step of the proton uptake is the proton transfer from E286 to the catalytic site [33], the KIE of ~2 is presumably associated with this reaction. The observed pK_a in the pH dependence of this transition presumably reflects the apparent pK_a of E286 (or E286 including H_2O molecules around the site, see [56,57]), which acts as a transient internal proton donor to the catalytic site [33,52]. The relatively small KIE of the $P^3 \rightarrow F^3$ transition is typical of a proton transfer trough a hydrogen-bonded proton-transfer pathway. Furthermore, the pK_a of the pH/pD dependence of the transition rate changed from 9.4 in H_2O to 9.6 in D_2O where such a small pK_a increase is typical for e.g. carboxylates upon replacement of the H_2O solvent by a D_2O solvent [58].

Also in the DN132, ED286 and RK481 mutant Cyt*c*Os the $P^3 \rightarrow F^3$ transition displayed KIEs of 2–2.5. Because in the DN132 mutant Cyt*c*O there is no proton uptake from solution on the time scale of the $P^3 \rightarrow F^3$ transition and it involves internal proton transfer to the catalytic site, observation of a KIE of ~2 in the mutant Cyt*c*O is consistent with the notion that proton transfer from E286 to the catalytic site is the rate-limiting step of the $P^3 \rightarrow F^3$ transition. Furthermore, the results show that neither alteration of the internal proton donor (ED286) nor alteration of a group that is presumably involved in proton release (RK481) have any effects on the KIE (see Table 1). Together, these results indicate that the same proton-transfer event is rate determining in H_2O and D_2O in the wild-type as well as in mutant Cyt*c*Os in which proton-transfer rates are altered. These data suggest that the $P^3 \rightarrow F^3$ transition is rate-limited by a "simple" proton-transfer reaction to the catalytic site and it is not controlled or rate limited by the uptake or release of pumped protons.

4.2. The $F^3 \rightarrow O^4$ transition in wild-type CytcO

The $F^3 \rightarrow O^4$ transition involves electron transfer from heme *a* to the catalytic site, proton transfer to the catalytic site, proton transfer to the pump site, and release of the pumped proton from the pump site. Thus, the difference between the $F^3 \rightarrow O^4$ transition and the $P^3 \rightarrow F^3$ transition discussed above is that only the former involves electron transfer to the catalytic site. Consequently, the $F^3 \rightarrow O^4$ transition is representative of any transition step during Cyt*c*O turnover, where electrons are delivered one-by-one, via Cu_A and heme *a* to the catalytic site. Results from earlier studies showed that in H_2O all internal electron and proton transfers during the $F^3 \rightarrow O^4$ transition occur with the same observed rates [44]. It should also be noted that the KIE is significantly larger for the $F^3 \rightarrow O^4$ than for the $P^3 \rightarrow F^3$ transition at pH 7.5, which indicates that different reactions determine the rates of these transitions.

The pH dependence of the $F^3 \rightarrow O^4$ transition rate in H_2O is determined by the protonation state of two titratable groups, one with a pK_a of 8.9 presumably E286 (as in the $P^3 \rightarrow F^3$ transition discussed above) and one with a pK_a <6 presumably the heme a_3/R481 cluster [18]. In D_2O, however, the rate of the $F^3 \rightarrow O^4$ transition titrates with only one pK_a of 6.7. This difference in the pH-dependencies could be due to a shift of the high pK_a from 8.9 to 6.7, and of the lower pK_a to a pH-region outside the measured pH range. However, a pK_a-shift of two units for a protein-derived proton donor (E286) is difficult to account for considering that protonatable groups shift their pK_as typically by ~0.5 units when moved from H_2O to D_2O [58]. Therefore, a more likely explanation is that the rate-limiting steps are different in H_2O and D_2O. One possibility is that the rate-limiting step of the $F^3 \rightarrow O^4$ transition involves two consecutive reaction steps displaying different KIEs such that one reaction is rate limiting in H_2O while the other is rate limiting in D_2O [44]. In a recent study we found that during the $F^3 \rightarrow O^4$ transition the electron-transfer rate to the catalytic site is determined by release of a pumped proton and/or a structural change linked to the release [44]. Hence, we speculate that one of these events could determine the rate of the transition in H_2O, while the other could determine the rate in D_2O.

4.3. Kinetic deuterium isotope effect of the $F^3 \rightarrow O^4$ transition rate in mutant CytcOs in which either electron or proton transfer is slowed

Results from an earlier study showed that even if the $F^3 \rightarrow O^4$ transition was slowed by a factor of ~100 (ML263 mutant Cyt*c*O [59]), due to slowed electron transfer, the KIE was the same as that observed with the wild-type Cyt*c*O (~8 at pH 7.5) [22], which indicates that the slowed electron transfer into the catalytic site does not alter the rate-limiting step of the $F^3 \rightarrow O^4$ transition. Also in the DN132 mutant Cyt*c*O the $F^3 \rightarrow O^4$ transition was slowed to approximately the same degree as in the ML263 mutant Cyt*c*O (from ~700 s^{-1} to ~2 s^{-1} at pH 7) (see Fig. 2C). However, in the DN132 mutant Cyt*c*O the rate is limited by proton uptake from solution rather then by electron transfer. In this case the $F^3 \rightarrow O^4$ transition displayed a KIE of only ~1.5 (see Fig. 2C). Thus, when proton uptake into the D pathway is rate-limiting the rate of the $F^3 \rightarrow O^4$ transition is essentially insensitive to replacement of H_2O by D_2O.

In summary, from the discussion above we conclude that even if the electron transfer is slowed by a factor of 100 (ML263 mutant Cyt*c*O) it is still controlled by the same proton transfer (a large KIE is observed). Only when proton transfer is rate limiting (DN132 mutant Cyt*c*O) the KIE decreases. A relevant question in this context is the identity of the proton transfer controlling the rate of the electron transfer associated with the $F^3 \rightarrow O^4$ transition. As discussed above, the transition is linked to proton uptake to the catalytic site and the uptake and release of the pumped proton. Because proton transfer to the catalytic site displays a small KIE of ~2 (see above discussion of the events associated with the $P^3 \rightarrow F^3$ transition), we conclude that the $F^3 \rightarrow O^4$ transition rate is determined by transfer of the pumped proton beyond E286, presumably on the "release side". That the proton release is the slowest reaction during a proton-pumping event was also found from studies of the kinetics of electron and proton transfer reactions upon injection of an electron into the oxidized Cyt*c*O [60].

4.4. Kinetic deuterium isotope effect of the $F^3 \rightarrow O^4$ transition in CytcOs where the E286/R481 region has been modified

The E286 and R481 residues are both located in a proposed proton-gating region of the Cyt*c*O [10,21,61–65]. In both the ED286 and the RK481 mutant Cyt*c*Os the KIE of the $F^3 \rightarrow O^4$ transition was ~2.5, i.e. smaller than that with the wild-type Cyt*c*O. As a consequence, in D_2O in a large fraction of the pH range the transition is *faster* in the mutant Cyt*c*Os than in the wild-type enzyme (c.f. Fig. 2B and Figs. 2D and E). In addition, the titration with a pK_a of <6, observed with the wild-type Cyt*c*O, was not present in the mutant Cyt*c*Os. In this context, we note that the relatively large KIE observed at low pH with the wild-type Cyt*c*O is mainly due to the increase in rate with decreasing pH in H_2O (the pK_a <6 titration). Thus, the reason for the smaller KIE observed with the ED286 and RK481 mutant Cyt*c*Os may be the missing low-pH titration.

On the basis of studies with the RK481 mutant Cyt*c*O, we previously proposed that the pK_a <6 titration is associated with the R481-heme a_3 D-propionate cluster [18]. The ED286 mutant Cyt*c*O, and to a lesser extent also the RK481 mutant enzyme, display shifts in the pH dependence of the $F^3 \rightarrow O^4$ transition to a lower pK_a value in D_2O as compared to H_2O (from 8.5 to 7.4 and from 8.8 to 8.7 for the ED286 and RK481 mutant Cyt*c*Os, respectively). Such pK_a shifts are unexpected because typically the affinity of a protonatable site for deuterons is higher than that for protons and, as a result the pK_a of a titratable group increases upon changing the solvent from H_2O to D_2O [58,66]. The observation of a lowered pK_a in D_2O indicates that the rate-limiting step is not the same in these mutant Cyt*c*Os as compared to the wild-type Cyt*c*O. The similarity in the pH-dependencies and the KIEs of the ED286 and RK481 mutant Cyt*c*Os suggests that residues E286 and R481 are mechanistically linked, which is consistent with the notion that this region of the enzyme is involved in controlling transfer of the pumped protons and thus the electron transfer to the catalytic site (see above).

Ferguson-Miller, Mills and colleagues found that in the presence of a membrane potential the R481K mutant Cyt*c*O has a much lower activity than that of the wild-type Cyt*c*O under the same conditions resulting in an unusually high respiratory-control ratio (RCR) [67,68]. These results suggest that residue R481 interacts with the proton-release site, e.g. the heme a_3 D-propionate [68], and supports the conclusion from this work that proton release (c.f. the protonation state of the proton-release site) determines the rate of electron transfer to the catalytic site. Furthermore, Ferguson-Miller and Mills also suggested that deprotonation of the propionates could be rate limiting and give rise to the large KIE of the electron transfer, linked to proton pumping (c.f. $F^3 \rightarrow O^4$ transition studied here). This KIE would be smaller if another reaction becomes rate limiting such as

proton transfer from D286 to the heme propionate in the ED286 mutant Cyt*c*O [68].

4.5. Structural changes of the E286/pump site-region

The X-ray crystal structure of the ED286 mutant Cyt*c*O (Fig. 3) indicates that an additional water molecule may be present in the cavity below D286, and that the hydrogen bond between residue 286 and the carbonyl oxygen of M107, seen in the wild-type Cyt*c*O structure, is broken. The shorter side chain of the Asp as compared to the Glu alters the hydrogen-bonding pattern and might result in higher flexibility of the segment stretching from M107 to R481. This would explain the increased $F^3 \rightarrow O^4$ rate in D_2O relative to the wild-type Cyt*c*O. It should be pointed out that the ED286 mutant Cyt*c*O pumps protons also in D_2O, i.e. the shorter and presumably more flexible side-chain does not affect the proton-pumping machinery. In this context it is interesting to note that among oxidases sequenced to date there is no example of an enzyme carrying this specific substitution (R. B. Gennis, personal communication). Therefore, it is likely that exchanging the Glu residue at position 286 in Cyt*c*O for an Asp imposes a functional disadvantage to the organism. A negative effect of the mutation might be manifested, for example, only when the enzyme works against an electrochemical potential across the membrane.

Acknowledgements

We would like to thank Shelagh Ferguson-Miller and Robert B. Gennis for providing the mutant strains of *Rhodobacter sphaeroides*. In a recent study, using ATR-FTIR spectroscopy, Gorbikova et al. (Biochemistry 46 (2007) 13141–13148), confirmed our proposal ([32] and discussion in this work) that Glu286 is an internal proton donor to the catalytic site.

References

[1] D.A. Mills, S. Ferguson-Miller, Understanding the mechanism of proton movement linked to oxygen reduction in cytochrome *c* oxidase: lessons from other proteins, FEBS Lett. 545 (2003) 47–51.
[2] P. Brzezinski, Redox-driven membrane-bound proton pumps, Trends Biochem. Sci. 29 (2004) 380–387.
[3] R.B. Gennis, Coupled proton and electron transfer reactions in cytochrome oxidase, Front. Biosci. 9 (2004) 581–591.
[4] M. Wikström, Cytochrome c oxidase: 25 years of the elusive proton pump, Biochim. Biophys. Acta 1655 (2004) 241–247.
[5] M. Brunori, A. Giuffre, P. Sarti, Cytochrome c oxidase, ligands and electrons, J. Inorg. Biochem. 99 (2005) 324–336.
[6] P. Brzezinski, P. Ädelroth, Design principles of proton-pumping haem-copper oxidases, Curr. Opin. Struct. Biol. 16 (2006) 465–472.
[7] S. Papa, G. Capitanio, P. Luca Martino, Concerted involvement of cooperative proton–electron linkage and water production in the proton pump of cytochrome *c* oxidase, Biochim. Biophys. Acta, Bioenerg. 1757 (2006) 1133–1143.
[8] S. Yoshikawa, K. Muramoto, K. Shinzawa-Itoh, H. Aoyama, T. Tsukihara, K. Shimokata, Y. Katayama, H. Shimada, Proton pumping mechanism of bovine heart cytochrome *c* oxidase, Biochim. Biophys. Acta, Bioenerg. 1757 (2006) 1110–1116.
[9] J. Quenneville, D.M. Popovic, A.A. Stuchebrukhov, Combined DFT and electrostatics study of the proton pumping mechanism in cytochrome *c* oxidase, Biochim. Biophys. Acta, Bioenerg. 1757 (2006) 1035–1046.
[10] J.P. Hosler, S. Ferguson-Miller, D.A. Mills, Energy transduction: proton transfer through the respiratory complexes, Ann. Rev. Biochem. 75 (2006) 165–187.
[11] S. Iwata, C. Ostermeier, B. Ludwig, H. Michel, Structure at 2.8 Å resolution of cytochrome *c* oxidase from *Paracoccus denitrificans*, Nature 376 (1995) 660–669.
[12] M. Svensson-Ek, J. Abramson, G. Larsson, S. Törnroth, P. Brzezinski, S. Iwata, The X-ray crystal structures of wild-type and EQ(I-286) mutant cytochrome *c* oxidases from *Rhodobacter sphaeroides*, J. Mol. Biol. 321 (2002) 329–339.
[13] T. Tsukihara, H. Aoyama, E. Yamashita, T. Tomizaki, H. Yamaguchi, K. Shinzawa-Itoh, R. Nakashima, R. Yaono, S. Yoshikawa, The whole structure of the 13-subunit oxidized cytochrome *c* oxidase at 2.8 Å, Science 272 (1996) 1136–1144.
[14] K. Shimokata, Y. Katayama, H. Murayama, M. Suematsu, T. Tsukihara, K. Muramoto, H. Aoyama, S. Yoshikawa, H. Shimada, The proton pumping pathway of bovine heart cytochrome *c* oxidase, Proc. Natl. Acad. Sci. U. S. A. 104 (2007) 4200–4205.
[15] A.A. Konstantinov, S. Siletsky, D. Mitchell, A. Kaulen, R.B. Gennis, The roles of the two proton input channels in cytochrome *c* oxidase from *Rhodobacter sphaeroides* probed by the effects of site-directed mutations on time-resolved electrogenic intraprotein proton transfer, Proc. Natl. Acad. Sci. U. S. A. 94 (1997) 9085–9090.
[16] P. Brzezinski, P. Ädelroth, Pathways of proton transfer in cytochrome *c* oxidase, J. Bioenerg. Biomembranes 30 (1998) 99–107.
[17] M. Wikström, A. Jasaitis, C. Backgren, A. Puustinen, M.I. Verkhovsky, The role of the D- and K-pathways of proton transfer in the function of the haem-copper oxidases, Biochim. Biophys. Acta 1459 (2000) 514–520.
[18] G. Brändén, M. Brändén, B. Schmidt, D.A. Mills, S. Ferguson-Miller, P. Brzezinski, The protonation state of a heme propionate controls electron transfer in cytochrome *c* oxidase, Biochemistry 44 (2005) 10466–10474.
[19] M.H. Olsson, P.E. Siegbahn, M.R. Blomberg, A. Warshel, Exploring pathways and barriers for coupled ET/PT in cytochrome *c* oxidase: a general framework for examining energetics and mechanistic alternatives, Biochim. Biophys. Acta 1767 (2007) 244–260.
[20] I. Hofacker, K. Schulten, Oxygen and proton pathways in cytochrome *c* oxidase, Proteins 30 (1998) 100–107.
[21] A. Puustinen, M. Wikström, Proton exit from the heme-copper oxidase of *Escherichia coli*, Proc. Natl. Acad. Sci. U. S. A. 96 (1999) 35–37.
[22] P. Ädelroth, M. Karpefors, G. Gilderson, F.L. Tomson, R.B. Gennis, P. Brzezinski, Proton transfer from glutamate 286 determines the transition rates between oxygen intermediates in cytochrome *c* oxidase, Biochim. Biophys. Acta 1459 (2000) 533–539.
[23] A. Namslauer, A.S. Pawate, R.B. Gennis, P. Brzezinski, Redox-coupled proton translocation in biological systems: proton shuttling in cytochrome *c* oxidase, Proc. Natl. Acad. Sci. U. S. A. 100 (2003) 15543–15547.
[24] T. Tsukihara, K. Shimokata, Y. Katayama, H. Shimada, K. Muramoto, H. Aoyama, M. Mochizuki, K. Shinzawa-Itoh, E. Yamashita, M. Yao, Y. Ishimura, S. Yoshikawa, The low-spin heme of cytochrome *c* oxidase as the driving element of the proton-pumping process, Proc. Natl. Acad. Sci. U. S. A. 100 (2003) 15304–15309.
[25] D.M. Popovic, A.A. Stuchebrukhov, Proton pumping mechanism and catalytic cycle of cytochrome *c* oxidase: Coulomb pump model with kinetic gating, FEBS Lett. 566 (2004) 126–130.
[26] J. Quenneville, D.M. Popovic, A.A. Stuchebrukhov, Combined DFT and electrostatics study of the proton pumping mechanism in cytochrome *c* oxidase, Biochim. Biophys. Acta 1757 (2006) 1035–1046.
[27] G. Brändén, R.B. Gennis, P. Brzezinski, Transmembrane proton translocation by cytochrome *c* oxidase, Biochim. Biophys. Acta 1757 (2006) 1052–1063.
[28] K. Faxén, G. Gilderson, P. Ädelroth, P. Brzezinski, A mechanistic principle for proton pumping by cytochrome *c* oxidase, Nature 437 (2005) 286–289.
[29] D. Zaslavsky, A.D. Kaulen, I.A. Smirnova, T. Vygodina, A.A. Konstantinov, Flash-induced membrane potential generation by cytochrome *c* oxidase, FEBS Lett. 336 (1993) 389–393.
[30] M.I. Verkhovsky, J.E. Morgan, M.L. Verkhovskaya, M. Wikström,

Translocation of electrical charge during a single turnover of cytochrome-c oxidase, Biochim. Biophys. Acta 1318 (1997) 6–10.
[31] D. Bloch, I. Belevich, A. Jasaitis, C. Ribacka, A. Puustinen, M.I. Verkhovsky, M. Wikström, The catalytic cycle of cytochrome *c* oxidase is not the sum of its two halves, Proc. Natl. Acad. Sci. U. S. A. 101 (2004) 529–533.
[32] I.A. Smirnova, P. Ädelroth, R.B. Gennis, P. Brzezinski, Aspartate-132 in cytochrome *c* oxidase from *Rhodobacter sphaeroides* is involved in a two-step proton transfer during oxo-ferryl formation, Biochemistry 38 (1999) 6826–6833.
[33] A. Namslauer, A. Aagaard, A. Katsonouri, P. Brzezinski, Intramolecular proton-transfer reactions in a membrane-bound proton pump: the effect of pH on the peroxy to ferryl transition in cytochrome *c* oxidase, Biochemsitry 42 (2003) 1488–1498.
[34] M. Iwaki, A. Puustinen, M. Wikström, P.R. Rich, ATR-FTIR spectroscopy of the PM and F intermediates of bovine and *Paracoccus denitrificans* cytochrome *c* oxidase, Biochemistry 42 (2003) 8809–8817.
[35] R.M. Nyquist, D. Heitbrink, C. Bolwien, R.B. Gennis, J. Heberle, Direct observation of protonation reactions during the catalytic cycle of cytochrome *c* oxidase, Proc. Natl. Acad. Sci. U. S. A. 100 (2003) 8715–8720.
[36] D. Heitbrink, H. Sigurdson, C. Bolwien, P. Brzezinski, J. Heberle, Transient binding of CO to Cu-B in cytochrome *c* oxidase is dynamically linked to structural changes around a carboxyl group: a time-resolved step-scan Fourier transform infrared investigation, Biophys. J. 82 (2002) 1–10.
[37] N. Agmon, The Grotthuss Mechanism, Chem. Phys. Lett. 244 (1995) 456–462.
[38] T.E. Decoursey, Voltage-gated proton channels and other proton transfer pathways, Physiol. Rev. 83 (2003) 475–579.
[39] M. Karpefors, P. Ädelroth, A. Aagaard, I.A. Smirnova, P. Brzezinski, The deuterium isotope effect as a tool to investigate enzyme catalysis: proton-transfer control mechanisms in cytochrome *c* oxidase, Isr. J. Chem. 39 (1999) 427–437.
[40] S. Hallén, T. Nilsson, Proton transfer during the reaction between fully reduced cytochrome *c* oxidase and dioxygen: pH and deuterium isotope effects, Biochemistry 31 (1992) 11853–11859.
[41] R.C. Sadoski, D. Zaslavsky, R.B. Gennis, B. Durham, F. Millett, Exposure of bovine cytochrome *c* oxidase to high triton X-100 or to alkaline conditions causes a dramatic change in the rate of reduction of compound F, J. Biol. Chem. 276 (2001) 33616–33620.
[42] D. Zaslavsky, R.C. Sadoski, K.F. Wang, B. Durham, R.B. Gennis, F. Millett, Single electron reduction of cytochrome *c* oxidase compound F: resolution of partial steps by transient spectroscopy, Biochemistry 37 (1998) 14910–14916.
[43] S.A. Siletsky, A.S. Pawate, K. Weiss, R.B. Gennis, A.A. Konstantinov, Transmembrane charge separation during the ferryl-oxo→oxidized transition in a nonpumping mutant of cytochrome *c* oxidase, J. Biol. Chem. 279 (2004) 52558–52565.
[44] L. Salomonsson, K. Faxén, P. Ädelroth, P. Brzezinski, The timing of proton migration in membrane-reconstituted cytochrome *c* oxidase, Proc. Natl. Acad. Sci. U. S. A. 102 (2005) 17624–17629.
[45] M. Karpefors, P. Ädelroth, P. Brzezinski, Localized control of proton transfer through the D-pathway in cytochrome *c* oxidase: application of the proton-inventory technique, Biochemistry 39 (2000) 6850–6856.
[46] D.M. Mitchell, R.B. Gennis, Rapid purification of wildtype and mutant cytochrome *c* oxidase from *Rhodobacter sphaeroides* by Ni(2+)-NTA affinity chromatography, FEBS Lett. 368 (1995) 148–150.
[47] D.M. Mitchell, J.R. Fetter, D.A. Mills, P. Ädelroth, M.A. Pressler, Y. Kim, R. Aasa, P. Brzezinski, B.G. Malmström, J.O. Alben, G.T. Babcock, S. Ferguson-Miller, R.B. Gennis, Site-directed mutagenesis of residues lining a putative proton transfer pathway in cytochrome *c* oxidase from *Rhodobacter sphaeroides*, Biochemistry 35 (1996) 13089–13093.
[48] D.A. Mills, L. Geren, C. Hiser, B. Schmidt, B. Durham, F. Millett, S. Ferguson-Miller, An arginine to lysine mutation in the vicinity of the heme propionates affects the redox potentials of the hemes and associated electron and proton transfer in cytochrome *c* oxidase, Biochemistry 44 (2005) 10457–10465.
[49] M. Brändén, H. Sigurdson, A. Namslauer, R.B. Gennis, P. Ädelroth, P. Brzezinski, On the role of the K-proton transfer pathway in cytochrome *c* oxidase, Proc. Natl. Acad. Sci. U. S. A. 98 (2001) 5013–5018.
[50] Z. Otwinowski, W. Minor, Processing of X-ray diffraction data collected in oscillation mode, Methods Enzymol. 276 (1997) 307–326.
[51] M.D. Winn, M.N. Isupov, G.N. Murshudov, Use of TLS parameters to model anisotropic displacements in macromolecular refinement, Acta Crystallogr., D Biol. Crystallogr. 57 (2001) 122–133.
[52] A. Namslauer, P. Brzezinski, Structural elements involved in electron-coupled proton transfer in cytochrome *c* oxidase, FEBS Lett. 567 (2004) 103–110.
[53] J.R. Fetter, J. Qian, J. Shapleigh, J.W. Thomas, A. García-Horsman, E. Schmidt, J. Hosler, G.T. Babcock, R.B. Gennis, S. Ferguson-Miller, Possible proton relay pathways in cytochrome *c* oxidase, Proc. Natl. Acad. Sci. U. S. A. 92 (1995) 1604–1608.
[54] D.A. Mills, Z. Tan, S. Ferguson-Miller, J. Hosler, A role for subunit III in proton uptake into the D pathway and a possible proton exit pathway in *Rhodobacter sphaeroides* cytochrome *c* oxidase, Biochemistry 42 (2003) 7410–7417.
[55] K. Muramoto, K. Hirata, K. Shinzawa-Itoh, O.S. Yoko, E. Yamashita, H. Aoyama, T. Tsukihara, S. Yoshikawa, A histidine residue acting as a controlling site for dioxygen reduction and proton pumping by cytochrome *c* oxidase, Proc. Natl. Acad. Sci. U. S. A. 104 (2007) 7881–7886.
[56] A. Aagaard, G. Gilderson, D.A. Mills, S. Ferguson-Miller, P. Brzezinski, Redesign of the proton-pumping machinery of cytochrome *c* oxidase: proton pumping does not require Glu(I-286), Biochemistry 39 (2000) 15847–15850.
[57] C. Backgren, G. Hummer, M. Wikström, A. Puustinen, Proton translocation by cytochrome *c* oxidase can take place without the conserved glutamic acid in subunit I, Biochemistry 39 (2000) 7863–7867.
[58] R.L. Schowen, Solvent isotope effects on enzymic reactions, in: W.W. Cleland, M.H. O'Leary, D.B. Northrop (Eds.), Isotope Effects on Enzyme-Catalyzed Reactions, University Park Press, Baltimore, MD, 1977, pp. 64–99.
[59] M. Karpefors, P. Ädelroth, Y. Zhen, S. Ferguson-Miller, P. Brzezinski, Proton uptake controls electron transfer in cytochrome *c* oxidase, Proc. Natl. Acad. Sci. U. S. A. 95 (1998) 13606–13611.
[60] I. Belevich, D.A. Bloch, N. Belevich, M. Wikström, M.I. Verkhovsky, Exploring the proton pump mechanism of cytochrome *c* oxidase in real time, Proc. Natl. Acad. Sci. U. S. A. 104 (2007) 2685–2690.
[61] J. Behr, H. Michel, W. Mäntele, P. Hellwig, Functional properties of the heme propionates in cytochrome *c* oxidase from *Paracoccus denitrificans*. Evidence from FTIR difference spectroscopy and site-directed mutagenesis, Biochemistry 39 (2000) 1356–1363.
[62] P. Brzezinski, G. Larsson, Redox-driven proton pumping by heme-copper oxidases, Biochim. Biophys. Acta 1605 (2003) 1–13.
[63] H. Michel, The mechanism of proton pumping by cytochrome *c* oxidase, Proc. Natl. Acad. Sci. U. S. A. 95 (1998) 12819–12824.
[64] D.M. Popovic, A.A. Stuchebrukhov, Electrostatic study of the proton pumping mechanism in bovine heart cytochrome *c* oxidase, J. Am. Chem. Soc. 126 (2004) 1858–1871.
[65] M. Wikström, M.I. Verkhovsky, G. Hummer, Water-gated mechanism of proton translocation by cytochrome *c* oxidase, Biochim. Biophys. Acta 1604 (2003) 61–65.
[66] K.B. Schowen, R.L. Schowen, Solvent isotope effects on enzyme systems, Methods Enzymol. 87 (1982) 551–606.
[67] D.A. Mills, L. Florens, C. Hiser, J. Qian, S. Ferguson-Miller, Where is 'outside' in cytochrome *c* oxidase and how and when do protons get there? Biochim. Biophys. Acta 1458 (2000) 180–187.
[68] D.A. Mills, S. Ferguson-Miller, Influence of structure, pH and membrane potential on proton movement in cytochrome oxidase, Biochim. Biophys. Acta 1555 (2002) 96–100.